의학석사 학위논문

Correlation of Volumetric Perfusion CT Parameters with HIF-1 alpha Expression in Rabbit VX2 Tumor Model

토끼 등근육에 유발한 VX2 종양 모델에서 HIF-1α 발현과 관류 CT 측정 지수와의 상관관계 연구

2013 년 02 월

서울대학교 대학원

의학과 영상의학전공

김 정 임

A thesis of the Master’s degree

토끼 등근육에 유발한 VX2 종양 모델에서 HIF-1α 발현과 관류 CT 측정 지수와의 상관관계 연구

Correlation of Volumetric Perfusion CT Parameters with HIF-1 alpha Expression in a VX2 Tumor Rabbit Model

February 2013

The Department of Radiology,
Seoul National University
College of Medicine
Jung Im Kim

ABSTRACT

Introduction: Angiogenesis is essential for tumor growth and adaptation to hypoxia of the tumor. Hypoxia inducible factor-1alpha (HIF-1α), a major regulator of adaptation to hypoxic stress, facilitates tumoral angiogenesis, growth and aggressive tumoral behavior such as invasion or metastasis. HIF-1α overexpression relates with increase of disease mortality and resistance to chemo- or radiation therapy. Perfusion CT is one of feasible techniques to evaluate tumor vascularity and it provides regional maps and quantitative measurements of various hemodynamic parameters of tumors. Therefore, the purpose of this study was to investigate the relationship between perfusion CT parameters and HIF-1α expression in a VX2 tumor rabbit model.

Methods: VX2 carcinoma tumors implanted in bilateral back muscle of 10 rabbits were evaluated with perfusion CT. Serial perfusion CT was performed on 7days, 10days and 14 days after tumor implantation. CT Perfusion data were analyzed to calculate blood flow (BF), blood volume (BV), and permeability of the whole tumor and the nonnecrotic peripheral area. These parameters were correlated with intratumoral HIF-1α

expression. For statistical analysis, Spearman rank correlation analysis and Mann-Whitney test were used.

Results: A total of 20 tumors were analyzed for HIF-1α expression. HIF-1α was expressed in twelve tumors; 2, 3 and 7 tumors were classified as score 1, 2 and 3. Five (5/6, 83.3%), 4 (4/6, 66.7%) and 3 (3/8, 37.5%) tumors were obtained on days 7, 10, and 14 after tumor implantation. Permeability of the whole tumor showed significant positive correlation with HIF-1α score ($r = 0.45$, $p < 0.05$). Permeability of the periphery showed more significant positive correlation with HIF-1α score ($r = 0.89$, $p < 0.001$). Permeability of HIF-1α positive group was significantly higher than HIF-1α negative group ($p < 0.05$; the whole tumor, $p < 0.001$; the periphery).

Conclusions: In VX2 tumor, HIF-1α expression positively correlated with permeability from perfusion CT imaging and the correlation of the periphery was stronger than the whole tumor. Perfusion CT can be used as surrogate marker in the surveillance of HIF-1α activity.

Keywords: Perfusion CT, HIF-1α, VX2

Student number: 2008-21882

CONTENTS

LIST OF TABLES AND FIGURES

LIST OF ABBREVIATIONS

HIF−1 α : Hypoxia inducible factor−1alpha

CT: Computed tomography

BV: Blood volume

BF: Blood flow

INTRODUCTION

Angiogenesis is essential for tumor growth, invasion, and metastasis. If neovascularization is absent, tumors cannot grow because oxygen lack in the center of the tumor results in apoptosis and necrosis. Therefore, cancer cells have to adapt themselves to hypoxia by several mechanisms (1, 2). Hypoxia inducible factor-1 alpha (HIF-1α) is a major regulator of cell adaptation to hypoxic stress and plays a critical role in angiogenesis. It is the oxygen-regulated subunit of HIF-1 and determines HIF-1 activity (3). HIF-1α controls the expression of more than 40 target genes that play crucial roles in angiogenesis, tumoral growth, erythropoiesis and biological events associated with aggressive tumor behavior such as invasion or metastasis (4). Clinical data indicate that HIF-1α overexpression is associated with increased risk of patient mortality in many cancers (5). Furthermore, a growing number of HIF-1α inhibitors for cancer therapy are in clinical trials or are already approved for the treatment of cancer or other diseases.

Perfusion computed tomography (CT) is a feasible technique to evaluate tumor vascularity. It is on the basis of the linear relationship between CT enhancement and iodinated contrast material concentration. Perfusion CT provides regional maps and quantitative measurements of various hemodynamic parameters such as tumor angiogenesis, blood perfusion, and vascular permeability (6-10). With the relatively recent development of multi-detector CT (MDCT) performing volume-based technique and the release of commercially available software packages, the application of perfusion CT to the study of various organs have increased (8, 11-16). Especially, a number of studies introduced perfusion CT as a monitoring modality of antiangiogenic therapy for various tumors (e.g., brain tumor, renal cell carcinoma, hepatocellular carcinoma, gastrointestinal cancer and prostate cancer) (17-21). Given that HIF-1α is critical for tumor angiogenesis, we hypothesized that perfusion parameters may be surrogate markers for expression of HIF-1α.

Thus, the purpose of this study was to assess the relationship between dynamic contrast-enhanced perfusion CT parameters and HIF-1α expression in a VX2 tumor rabbit model.

MATERIALS AND METHODS

1. Animal model

This study was approved by the animal care committee at our institute. The rationale for selecting the VX2 tumor as the experimental model is as follows. The blood supply is similar to that of human hepatocellular carcinoma, the tumor grows rapidly, and the tumor becomes a relatively large tumor that is easily identified by imaging (22-24). Ten adult New Zealand white rabbits weighing 3.0 to 3.5 kg each were used. A 24-gauge medicut was inserted into an auricular vein. Anesthesia was induced with intravenous ketamine hydrochloride (50 mg per kg of body weight; Ketamine, Yuhan, Korea) and 2% xylazine (0.1 mL/kg; Rompun, Bayer, Germany). The bilateral back parallel to spine of the rabbits was sterilized after shave and rabbits were positioned prone on the table. Under the ultrasound (US) guide, the 21-gauge Chiba needle was inserted into bilateral back muscle at the level of kidney. Then, a VX2 tumor suspension (0.1mL) was slowly injected into each back muscle through the Chiba needle. Finally, injection site marking was performed at the resultant 20 tumors for facilitation of tumor localization,

2. Perfusion CT examination

One week following tumor implantation when the tumors were expected to be round in shape with a 1cm diameter, perfusion CT scanning was performed in all 10 rabbits. For histopathologic comparison at the intermediate time points of 7 10 and 14 days after tumor implantation, three rabbits for each time point were sacrificed after CT imaging. Before CT scanning, anesthesia was induced as described above. Then, rabbits were fixed on a CT board in the supine position and a thoracoabdominal bandage was applied to reduce any movement artifacts.

All perfusion CT imaging were performed with a 64-detector row dual-source scanner (Siemens Definition; Siemens Medical Solutions, Erlangen, Germany). To localize the tumor, a noncontrast CT study (80 kV; 120 mAs; detector configuration, 20x0.6 mm; rotation time, 1 second; section thickness, 5.0 mm; reconstruction interval, 5.0 mm; reconstruction kernel, H31s) was performed for complete coverage of the tumor. The marking of the tumor injection site was a good guide to tumor localization. An experienced radiologist (J.I.K.) with three years of experience in chest perfusion CT analyzed the

unenhanced CT images and selected a fixed scanning range to cover the entire mass with care taken to avoid possible exclusion of the peripheral portion of the mass during free breathing.

A total of 6.5mL of nonionic iodinated contrast medium (Ultravist 370, Schering, Berlin, Germany) was injected using dual-phase injection protocol (3 mL at 0.5 mL/sec and 3.5 mL at 0.1 mL/sec followed by a 1.5 mL saline flush at 0.1 mL/ sec) and a dual-head power injector (MedradStellant Dual; Medrad, Indianola, Pa). Perfusion CT imaging was performed 2 seconds after injection with free-breathing dynamic acquisition. CT parameters were as follows: 120 kV, 150 mAs; detector configuration, 24x1.2 mm; rotation time, 0.33 second; section thickness, 3.0 mm; reconstruction interval, 2 mm; reconstruction kernel, B20f. Dynamic CT scans were obtained 40 times for each mass with a 1.5 second interval for the first 20 scans, a 3 second interval for the 10 scans and a 6 second interval for the remaining 10 scans. Total scanning time was 120 seconds.

3. Quantification of perfusion parameters

All reconstructed image data were transferred to a commercially available imaging workstation (CT workplace; Siemens, Germany). An experienced radiologist (J.I.K.) performed the measurement of perfusion parameters using commercial software (Syngo VPCT, Siemens Healthcare, Forchheim, Germany). The measurement was performed with computerized motion correction using whole tumor coverage. For this measurement, an automated three-dimensional motion correction algorithm featuring a previously described nonrigid registration model was applied to the perfusion datasets (25). Motion-corrected images were then used to calculate the perfusion parameters. Arterial input was measured by placing a circular region of interest within the abdominal aorta and an arterial time-enhancement curve was automatically generated with the software (Figure 1A, B, Figure 2A-D).

The volume of interest (VOI) of the whole tumor was drawn manually around the tumor outline in all three planes (axial, coronal, and sagittal) with exclusion of adjacent muscle (Figure 1A). The following settings were adopted for segmentation: tissue upper and lower limits of 150 and −50 HU, respectively, reference vessel input window width and a center of 300 and

150 HU, respectively, and percentage of relative threshold inside and outside of 50 and 50, respectively. The VOI of whole tumor was 1.06 ± 0.85 (0.17−3.01cm^3).

The second measurement was performed using smaller VOIs. Four VOIs were drawn manually at the periphery of the tumor; ROI ranged from 0.01 to 0.06 cm^3 with a mean value of 0.02 (± 0.01); a central necrotic low attenuated lesion and adjacent muscle or subcutaneous tissue were avoided as far as possible (Figure 1B). The average value of four VOIs was taken as the value of "periphery" of the tumor.

The quantification of perfusion parameters was performed forty−two times for 20 tumors (20 on days 7, 14 on days 10, and 8 on days 14 after tumor implantation). In each measurement of perfusion CT, blood flow (BF; ml/100 ml/min), blood volume (BV; ml/100 ml), and permeability (ml/100 ml/min) were obtained. In the software (Syngo VPCT, Siemens Healthcare, Forchheim, Germany) of this study, blood flow was calculated using the maximum slope method (26) and blood volume and permeability were calculated using Patlak analysis (27).

(A)

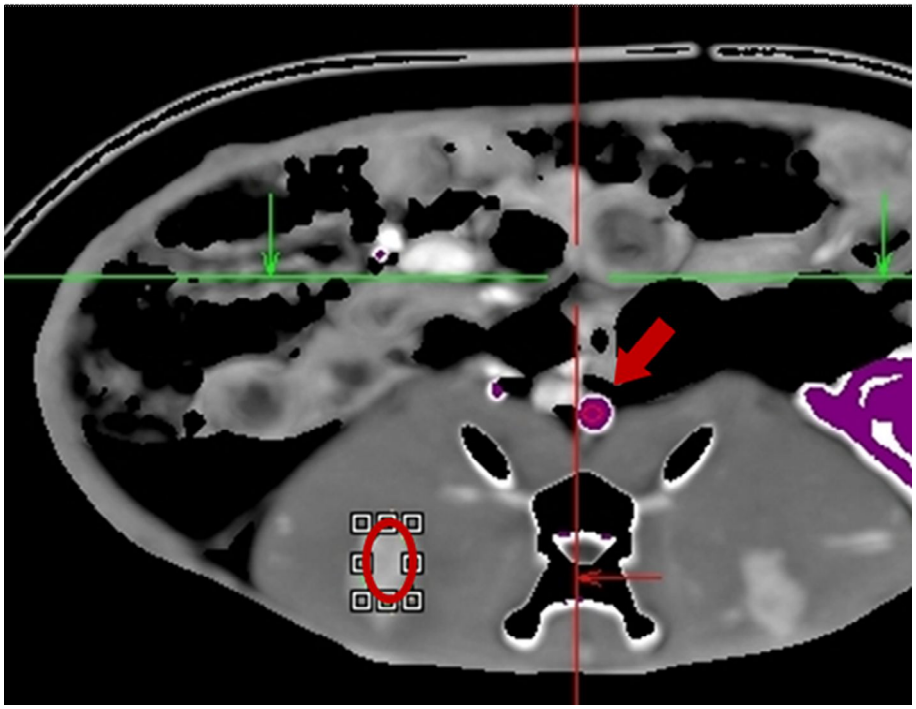

(B)

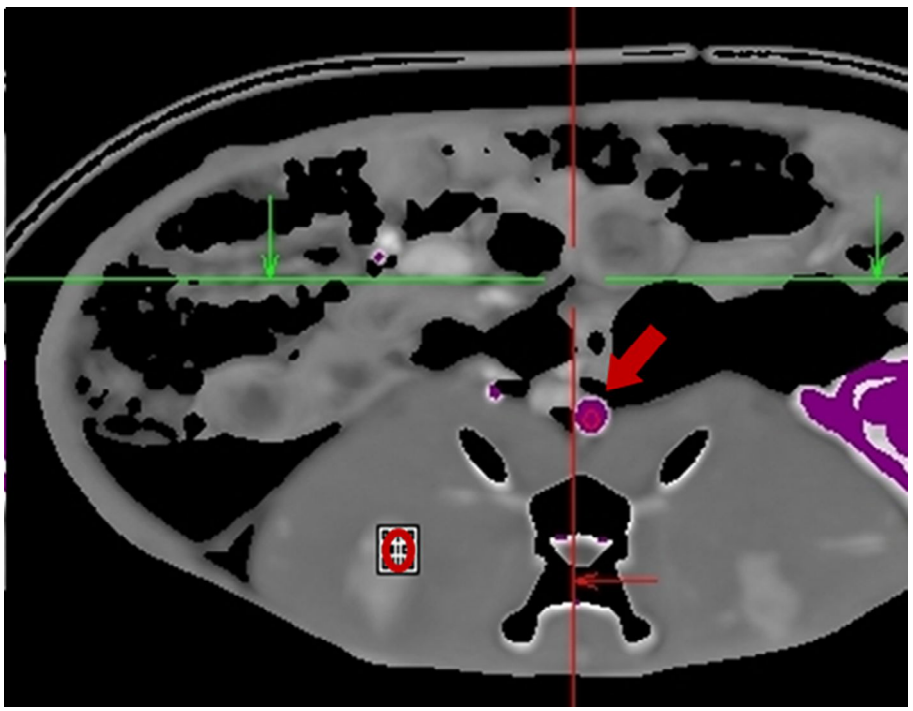

Figure 1. Quantification of perfusion parameters; step I.

Axial CT image shows VX2 tumors at bilateral back muscle. Circled areas in the tumors are volume of interest (VOI) (A) outlining visible tumor and (B) of the periphery. Four VOIs of the periphery were manually drawn on every tumor. Arrows indicates circular region of interest (ROI) of the abdominal aorta for calculation of automatic arterial time-enhancement curve.

(A)

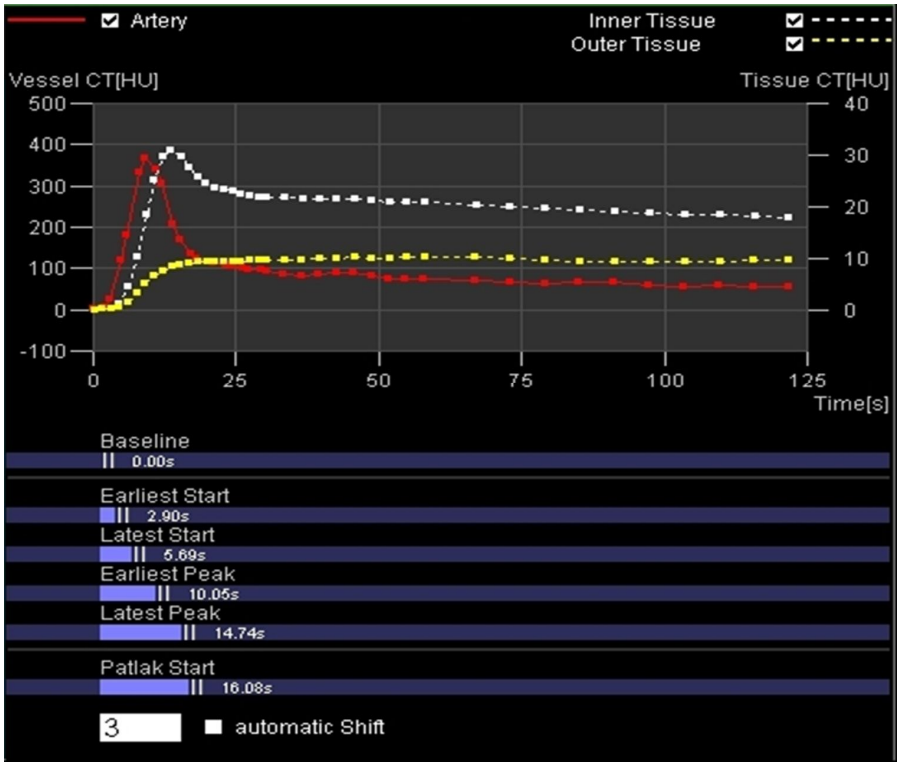
Artery
Inner Tissue
Outer Tissue
Vessel CT[HU]
Tissue CT[HU]
500
400
300
200
100
0
-100
40
30
20
10
0
0
25
50
75
100
125
Time[s]
Baseline
0.00s
Earliest Start
2.90s
Latest Start
5.69s
Earliest Peak
10.05s
Latest Peak
14.74s
Patlak Start
16.08s
3
automatic Shift

(B)

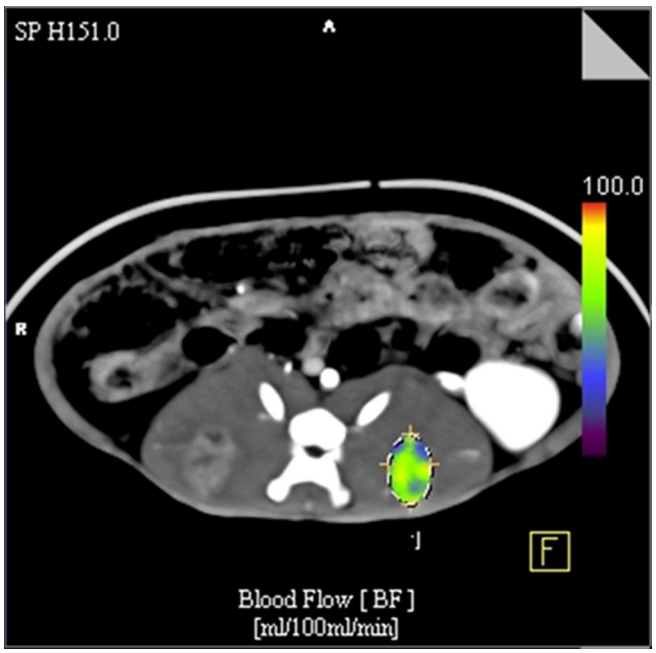
SP H151.0
A
100.0
R
F
Blood Flow [BF]
[ml/100ml/min]

(C)

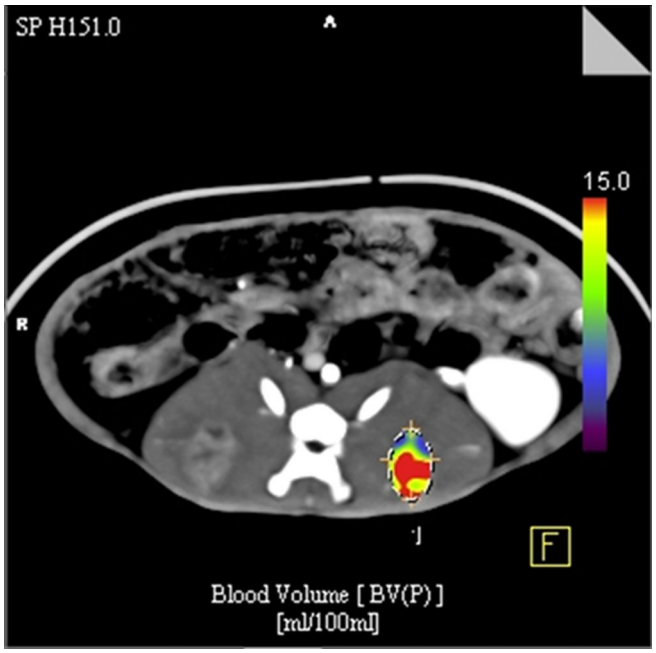
SP H151.0
A
15.0
R
F
Blood Volume [BV(P)]
[ml/100ml]

(D)

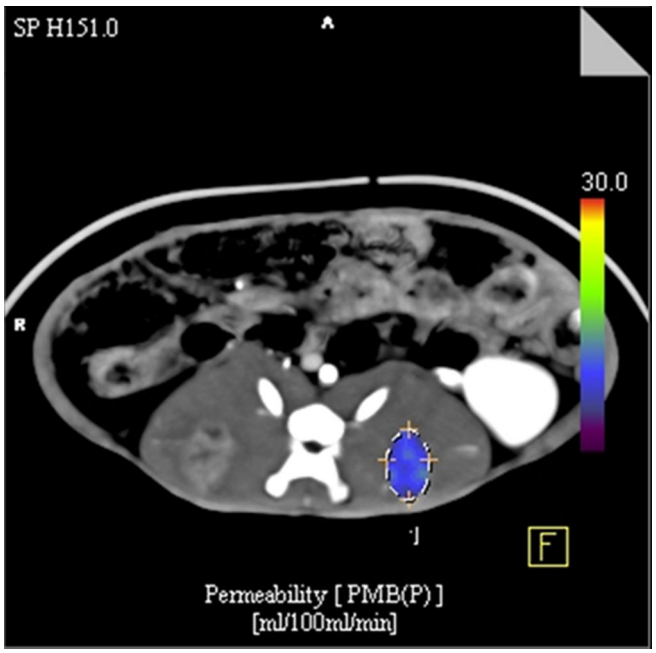
SP H151.0
A
30.0
R
F
Permeability [PMB(P)]
[ml/100ml/min]

Figure 2. Quantification of perfusion parameters; step II.

(A) Arterial time-enhancement curve of abdominal aorta. (B) Blood volume, (c) blood flow and (d) permeability parametric maps were obtained based on arterial time-enhancement curve.

4. Histopathologic evaluation

Immunohistochemical staining

Every perfusion CT scanning was completed, a transverse line at the skin of the rabbits was marked where the CT images had been obtained. Sacrificed rabbits were euthanized with an intravenous injection of a lethal amount of sodium thiopental (Pentothal) and were frozen in are refrigerator at −70° C in the position used for CT imaging. More than 24 hours later, rabbits were cut in the axial plane according to the guidance of the transverse line marked on the skin with 5 mm thickness. After each slice of the specimens was fixed with 10% phosphate−buffered formaldehyde and embedded in paraffin, pathologic specimens (approximately 5 μm thick) were obtained. Paraffin sections were dewaxed and washed with hydrogen peroxide for 5minutes and then rinsed gently with instilled water. The slides were then blocked with protein at room temperature for 5 minutes. These sections were stained with mouse anti-HIF−1α IgG2b monoclonal antibody (NB100 − 123, Novus Biologicals, Littleton, Colorado; dilution, 1:40,000) for 15 minutes. After15 minutes, slides were washed with freshly prepared Tris−Buffered Saline solution with Tween

(TBST) three times for 3-5 minutes each. Slides were then incubated with a secondary anti-mouse immunoglobulin-HRP and then washed with TBST solution three times for 3-5 minutes each (28). The sections were conterstained with hematoxylin and mounted.

Assessment of immunohistochemical staining

One pathologist (M.A.K.), who was blinded to the results of the perfusion CT scan, performed the histologic grading of HIF-1α. For evaluation of HIF-1α expression, at least five fields were randomly selected and a total of more than 1,000 tumor cells were microscopically counted under high magnification (400 x). The nuclear staining of the HIF-1α was predominant at the invading edge of the tumor border and at the periphery of necrotic areas within tumors (29). The HIF-1α expression was defined as positive if nuclear staining was observed in ≥5% of the tumor cells. Simultaneous cytoplasmic staining was excepted because nuclear HIF-1α determines the functional activity of the HIF-1α complex (Fig 3A, B) (30). According to the percentage of tumor cells stained, four categories were applied for grading of the HIF-1α expression: - (0-5%), 1+ (5-10%), 2+ (10-15%), 3+ (≥15%) (29).

(A)

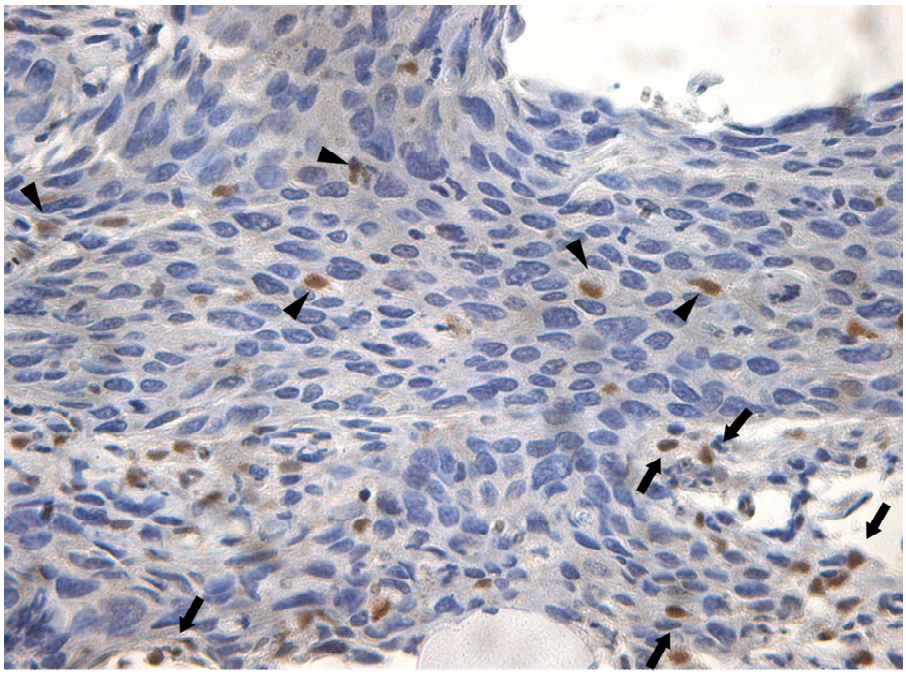

(B)

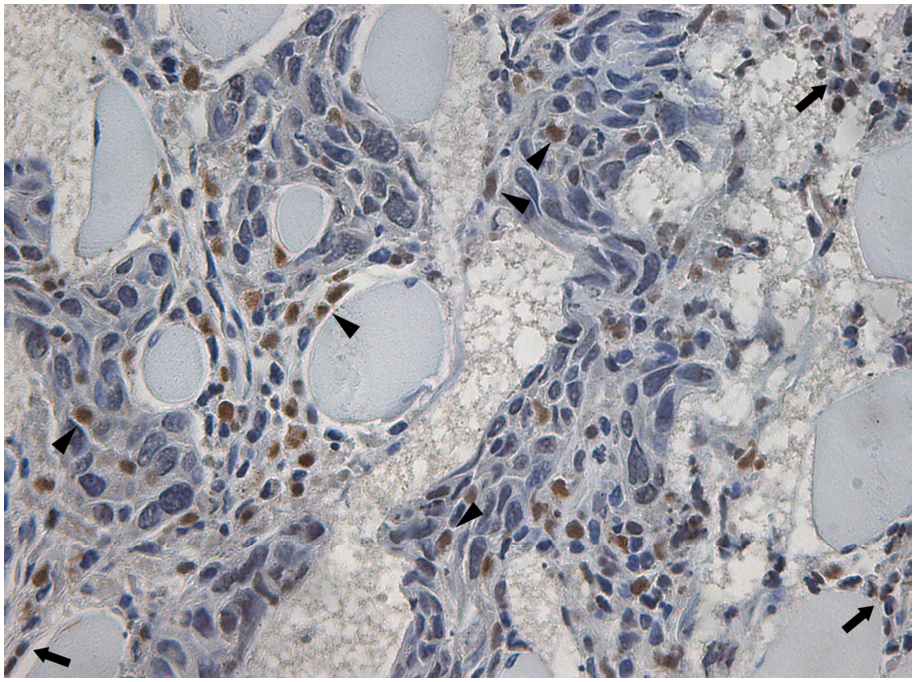

Figure 3. Immunoreactivity for hypoxia-inducible factor-1 alpha (HIF-1α) (A, B; X400).

HIF-1α is mainly identified as positive staining in the nucleus of cancer cells (arrowheads). Inflammatory cells adjacent to the cancer cells also express HIF-1α and they were excluded at scoring of HIF-1α expression (arrows); (A) A total of 24 from 276 cancer cells express HIF-1α (slide from the tumor with score 2) and (B) a total of 43 from 208 cancer cells express HIF-1α (slide from the tumor with score 3).

5. Statistical analysis

Statistical analysis was performed using SPSS version 18.0 software for Windows (SPSS Inc., Chicago, IL). The data were reported as the mean ± standard deviation. The association between each of the three perfusion parameters and HIF-1α score evaluated on histologic specimen was estimated by using the Spearman correlation coefficient. The difference in the VOI between HIF-1α positive and negative tumors were tested for significance with the Mann-Whitney test. A two-tailed P value of less than 0.05 was considered a statistically significant difference for all statistical analyses.

RESULTS

On days 7, 10 and 14 after tumor implantation, the volume of whole tumor significantly increased as duration of tumor implantation increased; 0.31 ± 0.15, 0.78 ± 0.31 and 1.85 ± 0.76 cm^3, respectively. Table 1 summarizes mean value of serial CT perfusion parameters at each time points. Both of the whole tumor and the periphery, BF and permeability showed trend of increase and decrease, respectively, as duration of tumor implantation increased. Both of the whole tumor and the periphery, difference of BV between each time points was diminutive. When perfusion parameters of the whole tumor were compared with that of the periphery, BV of the whole tumor was significantly higher than the periphery ($p < 0.001$; paired t-test). BF of the whole tumor was slightly higher than the periphery and permeability of whole tumor was similar with the periphery.

Table 1. Perfusion parameters and tumor volume of the whole tumor and periphery at each time point

	Whole Tumor			Periphery		
	7D (n=20)	10D (n=14)	14D (n=8)	7D (n=20)	10D (n=14)	14D (n=8)
Tumor volume (VOI, mm^3)	0.31±0.15	0.78±0.31	1.85±0.76			
Blood flow (ml/100ml/min)	43.75±23.66	48.2±16.0	58.06±11.17	45.60±22.37	47.46±11.29	73.96±15.62
Blood volume (ml/100ml)	16.46±5.49	17.45±6.56	17.52±2.15	17.50±5.45	22.76±6.16	20.44±2.80
Permeability (ml/100ml/min)	8.73±4.19	8.79±4.67	5.92±1.00	9.66±1.76	6.89±1.55	7.00±2.63

Note. Data are presented as mean ± standard deviation.

HIF-1α Expression

A total of twenty VX2 tumors were analyzed for HIF-1α expression using immunohistochemical staining; 6, 6 and 8 tumors were obtained on days 7, 10 and 14 after tumor implantation, respectively. HIF-1α was expressed in twelve tumors; 2, 3 and 7 tumors were classified as score 1, 2 and 3. Among HIF-1α positive tumors, 5 (5/6, 83.3%), 4 (4/6, 66.7%) and 3 (3/8, 37.5%) tumors were obtained on days 7, 10, and 14 after tumor implantation, respectively. HIF-1α expression decreased as the time after tumor implantation elapsed with not enough statistical significance ($p = 0.08$).

Correlation between HIF-1α Expression and Perfusion Parameters

Table 2 summarizes mean value of CT perfusion parameters according to the HIF-1α score. In the measurement of the whole tumor, there was statistically significant positive correlation between HIF-1α score and permeability ($r = 0.45$, $p < 0.05$). In measurement of the periphery, there was more significant positive correlation between HIF-1α score and permeability ($r = 0.89$, $p < 0.001$) (Fig. 4A). BF and BV

showed not considerable negative correlation with HIF−1α score (r = −0.04, p = 0.87, r = −0.21, p = 0.38, respectively; the whole tumor, r = −0.05, p = 0.84, r = −0.20, p = 0.39, respectively; the periphery).

In the HIF−1α positive group (n=12), BF, BV and permeability of the whole tumor was 50.14 ± 17.81, 16.20 ± 4.54, and 8.14 ± 3.25, respectively; BF, BV and permeability of the periphery was 57.40 ± 21.80, 19.23 ± 4.46, and 8.96 ± 1.36, respectively. In the HIF−1α negative group (n=8), BF, BV and permeability of the whole tumor was 48.79 ± 16.04, 16.04 ± 3.92, and 5.88 ± 1.01, respectively; BF, BV and permeability of the periphery was 59.74 ± 17.83, 19.87 ± 3.40, and 5.92 ± 0.84, respectively (Fig. 4B). Permeability of the HIF−1α positive group was significantly higher than the HIF−1α negative group ($p < 0.05$; the whole tumor, $P < 0.001$; the periphery). There was no significant difference of VOI between HIF−1α positive and negative group (p = 0.24; 0.87 ± 0.77, 1.35 ± 0.93, respectively).

Table 2. Perfusion parameters of the whole tumor and periphery according to HIF-1α score

	Whole Tumor				
HIF-1α score	0 (n=8)	1 (n=2)	2 (n=3)	3 (n=7)	*P*
Blood flow (ml/100ml/min)	48.78±16.03	63.86±23.56	29.81±8.45	54.94±12.99	0.87
Blood volume (ml/100ml)	16.04±3.91	20.7±3.18	18.63±4.92	13.88±3.47	0.37
Permeability (ml/100ml/min)	5.88±1.01	6.46±0.03	7.90±1.28	8.72±4.17	**< 0.05 (r= 0.45)**
	Periphery				
HIF-1α score	0 (n=8)	1 (n=2)	2 (n=3)	3 (n=7)	*P*
Blood flow (ml/100ml/min)	59.74±17.83	81.05±28.36	34.94±10.48	60.27±15.88	0.84
Blood volume (ml/100ml)	19.87±3.40	22.19±1.28	20.35±5.42	17.90±4.57	0.39
Permeability (ml/100ml/min)	5.92±0.84	7.43±0.81	8.53±0.64	9.59±1.34	**< 0.001 (r= 0.89)**

Note. Data are presented as mean ± standard deviation.

The data in parenthesis are Spearman correlation coefficient.

(A)

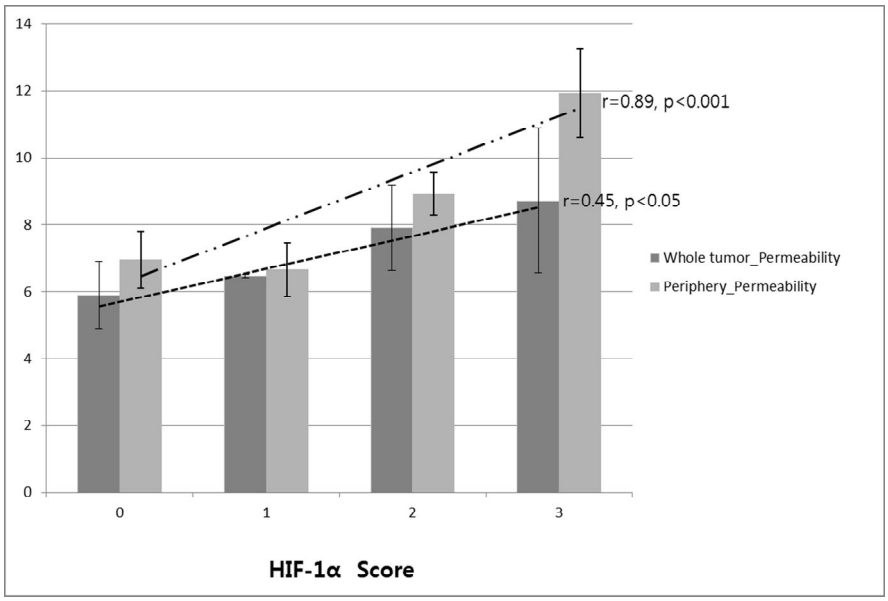
14
12
10
8
6
4
2
0
0
1
2
3
HIF-1α Score
r=0.89, p<0.001
r=0.45, p<0.05
Whole tumor_Permeability
Periphery_Permeability

(B)

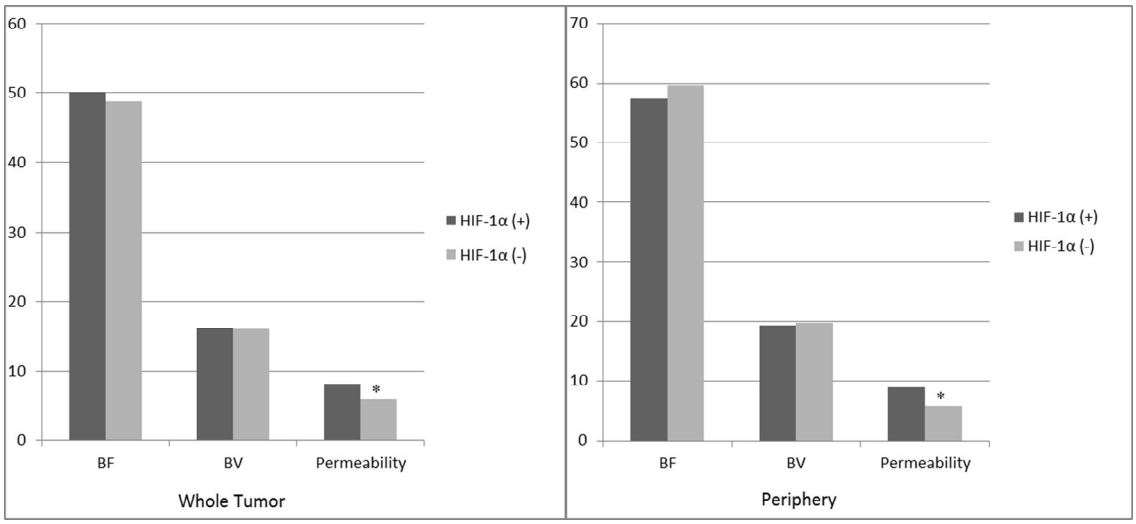
60
50
40
30
20
10
0
BF
BV
Permeability
*
Whole Tumor
HIF-1α (+)
HIF-1α (-)
70
60
50
40
30
20
10
0
BF
BV
Permeability
*
Periphery
HIF-1α (+)
HIF-1α (-)

Figure 4. Correlation of HIF-1α expression and perfusion parameters

(A) Permeability shows significant positive correlation with HIF-1α score by using a Spearman rank correlation. The correlation of HIF-1α score and permeability of the periphery is stronger than the whole tumor(r = 0.89, $p < 0.001$ vs. r = 0.45, $p < 0.05$, respectively). Error bars = standard deviation (B) BF and BV between HIF-1α positive (+) and negative (−) group are not substantially different. Permeability of the HIF-1α (+) group was significantly higher than the HIF-1α negative group ($p < 0.05$; the whole tumor, $P < 0.001$; the periphery).

DISCUSSION

Tumor angiogenesis is the system of organization of supplementary blood vessels from the preexisting ones. With the development of anti-angiogenic drugs that target inhibition of tumor angiogenesis, techniques that evaluate tumor angiogenesis have emphasized clinical practice. Intratumoral changes after this kind of treatment are important to recognize because in contrast to other anticancer therapies, such as use of cytotoxic agents and irradiation, a decrease in tumor volume is not an expected treatment response (31). There are several requisites for an optimal imaging technique to monitor therapy response: The method should be noninvasive and quantitative, sample the entire tumor, be quick to perform, and allow repetition at frequent interval (32). The perfusion CT has showed its possibility as a practical imaging modality to evaluate tumor vascularization.

HIF-1α activity in regions of intratumoral hypoxia mediates angiogenesis, epithelial-mesenchymal transition, stem-cell maintenance, invasion, metastasis, and resistance to radiation therapy and chemotherapy (5). A growing number of drugs have been identified that inhibit HIF activity by a variety of

molecular mechanisms and the clinical significant HIF −1α has highlighted for increase of the survival of cancer patient. Previous study showed that correlation of perfusion CT parameters and expression of microvessel density (MVD) or vascular endothelial growth factor (VEGF) in various tumors (5, 24, 33−35). In this study, we investigated the feasibility of perfusion CT as a noninvasive modality predicting HIF−1α expression in a VX2 tumor model.

Previous studies reported that there was no significant correlation between HIF−1α expression and tumor size (36−39). In this study, there was no statistically significant deference in volume of whole tumor between HIF−1α negative and positive group, suggesting poor effect of tumor size in expression of HIF−1α ($p = 0.24$). It can explain why the size of tumor cannot reflect the status of tumor perfusion or HIF−1α expression and why the perfusion parameters can be a more sensitive marker for anti−angiogenic therapy.

In this study, permeability increased in proportion to HIF−Iα expression and the correlation of the periphery was more significant than the whole tumor (Figure 4A). Moreover, permeability was significantly higher in HIF−1α positive group

than in HIF-1α negative group and the difference of the periphery were also more significant than the whole tumor. In the hypoxic condition, angiogenesis is activated at the edge of the tumor while the center progress tumor necrosis. This feature can explain predominant nuclear staining of the HIF-1α at periphery of tumor and stronger correlation with HIF-1α or more significant difference in permeability of the periphery between HIF-1α positive and negative group. Therefore, the perfusion parameters of the periphery relevantly reflected status of the tumor perfusion, although interobserver and intraobserver agreement of the periphery was poor than the whole tumor because of VOI size (40). For reduction of poor interobserver and intraobserver agreement of the periphery, this study used mean values of four VOIs in calculating perfusion parameters of the periphery.

There were some limitations in our study. First, we did not use any intervention developing direct tumor hypoxia. We assumed that tumor growth in itself caused tissue hypoxia and this study was performed under this hypothesis. The results of this study, no use of anti-angiogenic drug, is insufficient to apply at hypoxia resulted from antiangiogenic drug. Second, we

identified relationship between HIF-1α expression and perfusion parameters except for survey about prognostic effect of these relationships. However, we hope to this study can be a cornerstone that correlate perfusion parameter with HIF-1α expression in terms of anti-angiogenic treatment.

In conclusion, HIF-1α expression is related with increase of permeability and perfusion parameters can provide appropriate information about tissue perfusion. We hope that perfusion parameters can be a new surrogate marker of HIF-1α expression and can be a parameter predicting treatment response or prognosis of patients.

REFERENCES

1. Harris AL. Hypoxia—a key regulatory factor in tumour growth. Nature Reviews Cancer 2002;2:38-47
2. Aybatlı A, Sayın C, Kaplan PB, Varol F, Altaner Ş, Süt N. The investigation of tumoral angiogenesis with HIF-1 alpha and microvessel density in women with endometrium cancer. Journal of the Turkish-German Gynecological Association 2012;13
3. Wang GL, Jiang BH, Rue EA, Semenza GL. Hypoxia-inducible factor 1 is a basic-helix-loop-helix-PAS heterodimer regulated by cellular O2 tension. Proceedings of the national academy of sciences 1995;92:5510-5514
4. Zhong H, De Marzo AM, Laughner E, Lim M, Hilton DA, Zagzag D, et al. Overexpression of hypoxia-inducible factor 1α in common human cancers and their metastases. Cancer research 1999;59:5830-5835
5. Semenza GL. Hypoxia-inducible factors: mediators of cancer progression and targets for cancer therapy. Trends in pharmacological sciences 2012

6. Miles K. Perfusion CT for the assessment of tumour vascularity: which protocol? British Journal of Radiology 2003;76:S36-S42

7. Miles K. Functional CT imaging in oncology. European radiology 2003;13:M134

8. Miles K, Griffiths M. Perfusion CT: a worthwhile enhancement? British Journal of Radiology 2003;76:220-231

9. Park MS, Klotz E, Kim MJ, Song SY, Park SW, Cha SW, et al. Perfusion CT: Noninvasive Surrogate Marker for Stratification of Pancreatic Cancer Response to Concurrent Chemo-and Radiation Therapy1. Radiology 2009;250:110-117

10. Park CM, Goo JM, Lee HJ, Kim MA, Kim HC, Kim KG, et al. FN13762 Murine Breast Cancer: Region-by-Region Correlation of First-Pass Perfusion CT Indexes with Histologic Vascular Parameters1. Radiology 2009;251:721-730

11. Abe H, Murakami T, Kubota M, Kim T, Hori M, Kudo M, et al. Quantitative tissue blood flow evaluation of pancreatic tumor: comparison between xenon CT

technique and perfusion CT technique based on deconvolution analysis. Radiation medicine 2005;23:364

12. Cuenod CA, Leconte I, Siauve N, Resten A, Dromain C, Poulet B, et al. Early Changes in Liver Perfusion Caused by Occult Metastases in Rats: Detection with Quantitative CT1. Radiology 2001;218:556-561

13. Pandharipande PV, Krinsky GA, Rusinek H, Lee VS. Perfusion imaging of the liver: current challenges and future goals1. Radiology 2005;234:661-673

14. Sahani DV, Kalva SP, Hamberg LM, Hahn PF, Willett CG, Saini S, et al. Assessing Tumor Perfusion and Treatment Response in Rectal Cancer with Multisection CT: Initial Observations1. Radiology 2005;234:785-792

15. Goh V, Halligan S, Taylor SA, Burling D, Bassett P, Bartram CI. Differentiation between Diverticulitis and Colorectal Cancer: Quantitative CT Perfusion Measurements versus Morphologic Criteria—Initial Experience1. Radiology 2007;242:456-462

16. Sahani DV, Holalkere NS, Mueller PR, Zhu AX. Advanced Hepatocellular Carcinoma: CT Perfusion of Liver and

Tumor Tissue—Initial Experience1. Radiology 2007;243:736-743

17. Petralia G, Summers P, Viotti S, Montefrancesco R, Raimondi S, Bellomi M. Quantification of Variability in Breath-hold Perfusion CT of Hepatocellular Carcinoma: A Step toward Clinical Use. Radiology 2012

18. Jain R. Perfusion CT imaging of brain tumors: an overview. American Journal of Neuroradiology 2011;32:1570-1577

19. Osimani M, Bellini D, Di Cristofano C, Palleschi G, Petrozza V, Carbone A, et al. Perfusion MDCT of Prostate Cancer: Correlation of Perfusion CT Parameters and Immunohistochemical Markers of Angiogenesis. American Journal of Roentgenology 2012;199:1042-1048

20. Dighe S, Castellano E, Blake H, Jeyadevan N, Koh M, Orten M, et al. Perfusion CT to assess angiogenesis in colon cancer: technical limitations and practical challenges. British Journal of Radiology 2012;85:e814-e825

21. Reiner CS, Goetti R, Eberli D, Klotz E, Boss A, Pfammatter T, et al. CT perfusion of renal cell carcinoma: impact of volume coverage on quantitative analysis. Investigative radiology 2012;47:33

22. Park HS, Chung JW, Jae HJ, Kim YI, Son KR, Lee MJ, et al. FDG-PET for evaluating the antitumor effect of intraarterial 3-bromopyruvate administration in a rabbit VX2 liver tumor model. Korean Journal of Radiology 2007;8:216-224

23. Sun C, Liu C, Wang X, Chen J, Wang D, Merges R. Functional CT in a rabbit model: Evaluation of the perfusion characteristics before and after Ar-He cryoablation therapy. Journal of medical imaging and radiation oncology 2008;52:351-357

24. Choi SH, Chung JW, Kim HC, Baek JH, Park CM, Jun S, et al. The role of perfusion CT as a follow-up modality after transcatheter arterial chemoembolization: an experimental study in a rabbit model. Investigative radiology 2010;45:427-436

25. Saddi KA, Chefd' hotel C, Cheriet F. Large deformation registration of contrast-enhanced images with volume-preserving constraint. In, 2007; 651203

26. Miles K. Measurement of tissue perfusion by dynamic computed tomography. British Journal of Radiology 1991;64:409-412

27. Patlak CS, Blasberg RG, Fenstermacher JD. Graphical evaluation of blood-to-brain transfer constants from multiple-time uptake data. J Cereb Blood Flow Metab 1983;3:1-7

28. Virmani S, Rhee TK, Ryu RK, Sato KT, Lewandowski RJ, Mulcahy MF, et al. Comparison of hypoxia-inducible factor-1α expression before and after transcatheter arterial embolization in rabbit VX2 liver tumors. Journal of Vascular and Interventional Radiology 2008;19:1483-1489

29. Isobe T, Aoyagi K, Koufuji K, Shirouzu K, Kawahara A, Taira T, et al. Clinicopathological significance of hypoxia-inducible factor-1 alpha (HIF-1α) expression in gastric cancer. International Journal of Clinical Oncology 2012:1-12

30. Sherwood LM, Parris EE, Folkman J. Tumor angiogenesis: therapeutic implications. New England Journal of Medicine 1971;285:1182-1186

31. Hori K, Saito S, Sato Y, Akita H, Kawaguchi T, Sugiyama K, et al. Differential relationship between changes in tumour size and microcirculatory functions induced by therapy with an antivascular drug and with cytotoxic drugs: implications for the evaluation of therapeutic efficacy of AC7700 (AVE8062). European Journal of Cancer 2003;39:1957-1966

32. Thoeny HC, De Keyzer F, Chen F, Ni Y, Landuyt W, Verbeken EK, et al. Diffusion-weighted MR Imaging in Monitoring the Effect of a Vascular Targeting Agent on Rhabdomyosarcoma in Rats1. Radiology 2005;234:756-764

33. d'Assignies G, Couvelard A, Bahrami S, Vullierme MP, Hammel P, Hentic O, et al. Pancreatic Endocrine Tumors: Tumor Blood Flow Assessed with Perfusion CT Reflects Angiogenesis and Correlates with Prognostic Factors1. Radiology 2009;250:407-416

34. Bellomi M, Petralia G, Sonzogni A, Zampino MG, Rocca A. CT Perfusion for the Monitoring of Neoadjuvant Chemotherapy and Radiation Therapy in Rectal Carcinoma: Initial Experience1. Radiology 2007;244:486-493

35. Yao J, Yang Z, Chen H, Chen T, Huang J. Gastric adenocarcinoma: can perfusion CT help to noninvasively evaluate tumor angiogenesis? Abdominal imaging 2011;36:15-21

36. Vidal S, Horvath E, Kovacs K, Kuroki T, Lloyd R, Scheithauer B. Expression of hypoxia-inducible factor-1a (HIF-1a) in pituitary tumours 2003

37. Mabjeesh N, Amir S. Hypoxia-inducible factor (HIF) in human tumorigenesis. Histology and histopathology 2007;22:559

38. Hutchison GJ, Valentine HR, Loncaster JA, Davidson SE, Hunter RD, Roberts SA, et al. Hypoxia-Inducible Factor 1α Expression as an Intrinsic Marker of Hypoxia Correlation with Tumor Oxygen, Pimonidazole Measurements, and Outcome in Locally Advanced

Carcinoma of the Cervix. Clinical cancer research 2004;10:8405-8412

39. Maxwell P, Dachs G, Gleadle J, Nicholls L, Harris A, Stratford I, et al. Hypoxia-inducible factor-1 modulates gene expression in solid tumors and influences both angiogenesis and tumor growth. Proceedings of the national academy of sciences 1997;94:8104-8109

40. Goh V, Halligan S, Gharpuray A, Wellsted D, Sundin J, Bartram CI. Quantitative Assessment of Colorectal Cancer Tumor Vascular Parameters by Using Perfusion CT: Influence of Tumor Region of Interest1. Radiology 2008;247:726-732

국문 초록

서론: 종양의 신생혈관 생성은 종양의 성장 및 hypoxia 에 대한 종양의 적응에 중요한 역할을 한다. Hypoxia inducible factor-1alpha (HIF-1α)는 hypoxic stress 에 대한 주요 regulator 로서 종양의 혈관생성 및 전이나 침윤과 같은 종양의 공격성을 용이하게 한다. HIF-1α 과 발현은 항암치료나 방사선치료의 저항성 증가 및 환자의 mortality 증가와 관련이 높다.

Perfusion CT 는 종양의 vascularity 평가에 유용한 방법 중의 하나로 다양한 혈액역학 지수(blood volume (BV), blood flow (BF), permeability)들을 객관적으로 산출할 수 있어 antiangigenic 치료의 monitoring modality 로서도 주목 받고 있다.

Antiangiogenic 치료의 target 인 종양의 혈관생성에는 HIF-1α 가 결정적인 역할을 하며 현재 HIF-1α에 대한 연구는 활발히 진행되고 있으며 HIF-1α의 임상적 중요성은 커져가고 있다. 이 연구에서는 토끼의 VX2 tumor 모델에서 HIF-1α발현정도와 perfusion CT 지수 변화와의 상관관계 여부를 연구하고자 하였다.

방법:

연구자는 토끼의 양측 등에 VX2 tumor 를 이식한 후 7,10,14 일째 되는 날 perfusion CT 를 촬영하였다. 종양성장에 따른 HIF-1α발현 정도를 확인하기 위해 perfusion CT 촬영 후 각각 세 마리

의 토끼를 sacrifice 하였다. Perfusion CT 촬영후 전체 종양 및 종양의 가장자리에서 BV, BF, permeability 값을 계산하여 얻었다. 총 20 개의 tumor specimen 에 대하여 HIF-1α stain 을 하고 HIF-1α 발현을 4 단계로 나누었고 HIF-1α score 에 따른 perfusion CT 지수들의 변화에 대한 상관관계를 분석하였다.

결과: 20개의 종양 중 총 12개의 종양에서 HIF-1α발현을 확인하였고, 2,3, and 7개의 종양이 각각 score 1, score 2 and score 3로 판정되었다. 이중 5 (5/6, 83.3%), 4 (4/6, 66.7%) and 3 (3/8, 37.5%)개의 종양은 각각 종양 이식 후 7,10, 14일에 얻은 종양이었다. Permeability는 HIF-1α와 양의 상관관계를 보이며 periphery에서 얻은 값이 whole tumor보다 더 의미 있는 상관관계를 보였다 ($r = 0.45$, $p < 0.05$; the whole tumor, $r = 0.89$, $p < 0.001$: the periphery). HIF-1α양성 종양의 permeability가 HIF-1α음성 종양보다 유의하게 높으며 periphery에서 얻은 값이 좀 더 유의한 차이를 보였다 ($p < 0.05$; the whole tumor, $P < 0.001$; the periphery).

결론: 결론적으로 HIF-1α발현은 perfusion CT상 permeability와 양의 상관관계를 보이며 이러한 상관성은 periphery에서 얻은 값이 더 유의하다. 본 실험을 통해 perfusion CT가 HIF-1α activity 평가에 있어 surrogate marker가 될 수 있다는 가능성을 확인할 수 있었다.

주요어 : Perfusion CT, HIF-1 α, VX2

학 번 : 2008-21882